Chinese Journal of Chemical Engineering 76 (2024) 211–226

Contents lists available at ScienceDirect

Chinese Journal of Chemical Engineering

journal homepage: www.elsevier.com/locate/CJChE

Full Length Article

Rigorous design and economic optimization of reactive distillation column considering real liquid hold-up and hydraulic conditions of industrial device

Yuchang Du [1, 2], Yiqing Luo [1, 2, 3, *], Peilin Yang [1, 2], Shengkun Jia [1, 2, 3], Xigang Yuan [1, 2, 3]

[1] *Chemical Engineering Research Center, Tianjin University, Tianjin 300354, China*
[2] *School of Chemical Engineering and Technology, Tianjin University, Tianjin 300354, China*
[3] *State Key Laboratory of Chemical Engineering, Tianjin University, Tianjin 300354, China*

ARTICLE INFO

Article history:
Received 10 May 2024
Received in revised form
6 September 2024
Accepted 8 September 2024
Available online 5 October 2024

Keywords:
Reactive distillation
Liquid hold-up
Downcomer
Tray hydraulics
Pseudo-transient modeling method

ABSTRACT

The liquid hold-up in a reactive distillation (RD) column not only has a significant impact on the extent of reactions, but also affects the pressure drop and hydraulic conditions in the column. Therefore, the liquid hold-up would be a critical design factor for RD columns. However, the existing design methods for RD columns typically neglect the influence of considerable amount of liquid hold-up in downcomers owing to the difficulties of solving a large-scale nonlinear model system by considering downcomer hydraulics, resulting in significant deviations from actual situation and even operation infeasibility of the designed column. In this paper, a pseudo-transient (PT) RD model based on equilibrium model considering tray hydraulics was established for rigorous simulation and optimization of RD plate columns considering the liquid hold-up both in downcomers and column trays, and a steady-state optimization algorithm assisted by the PT model was adopted to robustly solve the optimization problem. The optimization results of either ethylene glycol RD or methyl acetate RD demonstrated that assuming all the liquid hold-up of a stage belonged to the tray will cause significant deviations in the column diameter, weir height, and the number of stages, which leads to not meeting the separation requirements and even operation hydraulic infeasibility. The rigorous model proposed in this study which considers the liquid hold-up both on trays and in downcomers as well as hydraulic constraints can be applied to systematically design industrial RD plate columns to simultaneously obtain optimal operating variables and equipment structure variables.

1. Introduction

Reactive distillation (RD) technology is one of the best success stories of the application of process intensification technology in chemical industry, which takes advantage of the synergies of the combination of reaction and separation to reduce energy requirements and capital cost, along with improving the sustainability of the distillation process [1,2]. Owing to the outstanding advantages and potential, the RD has attracted increasing attention from researchers in the field of chemical process intensification since the early 1920s [3]. Although the optimal design of RD columns based on rigorous model is necessary to yield optimal operating conditions with economic benefits, this is very difficult due to the large-scale nonlinear model equations that must be solved. In addition, because the RD is simultaneously affected by thermodynamic equilibrium and reaction kinetic or reaction equilibrium, the hydraulic condition in the RD column is crucial to achieve high reaction conversion and efficient separation. For example, the liquid hold-up at each column tray, which refers to certain of reaction volume, affects the extent of reactions, also significantly affects the pressure drop of the column tray, which thus affects the pressure and temperature distribution in the column, and subsequently affects the reaction kinetics or reaction equilibrium conditions and the phase equilibrium of components. Therefore, if these additional equations describing the real liquid hold-up and tray hydraulics are added to the RD model system, the scale and nonlinearity of the RD model will be further increased, and it will be more difficult to simultaneously optimize the operating variables and the structural variables of RD columns.

* Corresponding author.
E-mail address: luoyq@tju.edu.cn (Y. Luo).

https://doi.org/10.1016/j.cjche.2024.09.007

With the deepening understanding of RD, people have realized that the reasonable reaction volume is crucial to the optimal design and feasible operating of RD columns. Traditional design methods [4–7] for RD columns usually pre-specify the reaction volume (for liquid-phase reactions, this is usually the liquid hold-up on trays) of each stage according to the reaction kinetic conditions followed by repeatedly checking the hydraulics conditions in the column and adjusting the pre-specified volume setting to ensure the operation of the column is hydraulically feasible. Huss *et al.* [4] explored a hierarchy of methods and models for the design and simulation of the methyl acetate RD column by fixing the reaction volume of each column tray in reaction section as a large value of 3 m^3 with 23 in (1 in=25.4 mm) weir heights for the RD column. However, Li *et al.* [8] evaluated the results of Huss *et al.* by rigorous models considering tray hydraulics, and found serious weeping in the RD column, which meant the column cannot operate normally. Domingues *et al.* [9] designed a methyl *tert*-butyl ether (ETBE) catalytic distillation column by using a hybrid strategy coupled with evolutionary algorithm and nonlinear solver. The mass of the catalyst has a great influence on the design of catalytic distillation, and in this design, it was assumed that the mass of the catalyst used in each reaction stage is the same, that is, the reaction volume of the tray was fixed, which made the liquid hold-up of the tray cannot be in the best state. Tsatse *et al.* [7] presented a novel methodology for the simultaneously optimize the design and operation of complex reaction distillation processes, and considered multiple process alternatives. The fixed liquid hold-up was also adopted in the design, and the pressure drop of the tray was ignored. Although this work did not optimize the liquid hold-up, it explored the influence of different fixed values of liquid hold-ups on the optimal design under fast and slow reaction kinetics, and found that the system was more sensitive to changes in the liquid hold-up when the reaction kinetics was slow. In summary, improper design of reaction volume not only fails to optimize the design, but also may lead to poor hydraulic conditions in a column, making operation infeasible. Therefore, the liquid hold-ups should be taken as optimized variables under the constraints of hydraulic limitations and cannot be specified directly [10]. Li *et al.* [8] also evaluated the design result of ethylene glycol RD column by Ma *et al.* [11], who optimized the RD column by rigorous model, in which the reaction volume on each tray was taken as optimized variable but the tray hydraulics of pressure drop of each column tray was artificially specified. Similarly, a significant deviation from the actual pressure drop inevitably arose, and the obtained optimal reaction volume distribution in the reaction section of the RD column was practically impossible to achieve due to the hydraulic limitation of the column.

In addition, although the importance of considering tray hydraulic limitation to the design of RD column has been recognized, simplified methods which assume the liquid hold-up existing only on column trays, are typically adopted to reduce the scale and difficulty of problem modeling and solving, such as the study of Li *et al.* [8] and Noll *et al.* [12], based on the equilibrium stage model, used the tray pressure drop model to rigorous calculate the liquid hold-up of the tray, and took this parameter as an additional model output. Although this method accurately calculates the liquid hold-up in the tray, for homogeneous RD plate column, reactions not only occur in the liquid on column trays, but also in the liquid of downcomers. The assumption that the liquid phase completely exists on trays will inevitably lead to overestimations of the designed weir height, column diameter, or the number of trays, and eventually lead to unreasonable design and even infeasible operation because of hydraulic limitation. For heterogeneous RD, the catalyst is usually installed on the tray, so there is no reaction in the downcomer. However, ignoring the downcomer liquid hold-up will make the downcomer design lack of liquid volume parameters, and may also lead to unreasonable design or hydraulics infeasibility.

To describe the process of RD plate column more accurately and address the issue of excessive model complexity and computational difficulties, this study formulated a pseudo-transient (PT) equilibrium RD model considering the reactions in the liquid hold-ups of both downcomers and column trays, stage pressure drop and column hydraulics constraints, so as to achieve rigorous simulation of RD columns. By applying a steady-state optimization method assisted by the PT model, the simultaneous optimization of discrete variables of column structure and continuous operating variables was achieved, and the impact of liquid hold-up in downcomers on optimal design was further explored.

The remainder of this paper is structured as follows: in Section 2, the RD model considering the liquid hold-up in downcomers and the optimization algorithm are introduced. In Section 3, two cases of the ethanol glycol RD column and methyl acetate RD column, are used to demonstrate the influence of liquid hold-up in downcomers on the design of RD designs. Section 4 concludes the study.

2. Reactive Distillation Model and Optimization Algorithm

In an RD column, the ongoing reaction and separation process lead to strong coupling and nonlinearity in the large-scale RD model due to the mutual influence between component reaction and separation, as well as the mass transfer between the adjacent trays. Without good initial value estimation, existing nonlinear equations solving techniques cannot guarantee the convergence of the simulation problem. Therefore, the most significant challenge for rigorous optimization of an RD column is the robust and reliable solution of large-scale, strong coupled nonlinear equation models. For the rigorous simulation of complex processes, Pattison and Baldea [13] have shown that if the nonlinear equations in an algebraic equation model are reconstructed as differential equations, the reconstructed differential algebraic model can be solved based on the initial conditions of dynamic variables (rather than initial values), so that the convergence domain of the simulation problem can be effectively expanded and the same steady-state solution can be obtained as the original algebraic equation. Therefore, based on the concept of pseudo-transient continuation approach proposed by Pattison and Baldea [13] and the pseudo-transient modeling method, in this section an PT equilibrium RD model was established, in which the liquid hold-up on trays and in downcomers are considered separately.

Fig. 1 is the schematic diagram of an equilibrium stage in an RD column composed of a plate tray and downcomer, as shown by the area contained in the shadow in the figure. The liquid from the upper stage downcomer (flow rate L^{j-1}, and mole fraction x_i^{j-1}) flows into the tray j, and as the reactions and separation of components on the tray proceed, the liquid leaves the tray and enters the downcomer with a flow rate of L^j_{tray}, and a mole fraction of $x^j_{i,\text{tray}}$. If the catalyst is present, the reactions in the downcomer continue, and the flow rate of the liquid leaving the downcomer is L^j and mole fraction is x_i^j. To consider the liquid hold-up of a tray and its downcomer separately, following assumptions were adopted:

(1) The vapor and liquid streams at each tray are in thermodynamic equilibrium with one another when exiting the tray;
(2) The liquid hold-up in the downcomer is uniformly mixed, and the reactions can be still occurring for homogeneous catalysis;
(3) The vapor entrained by the liquid into the downcomer does not engage in mass transfer with the liquid, but solely

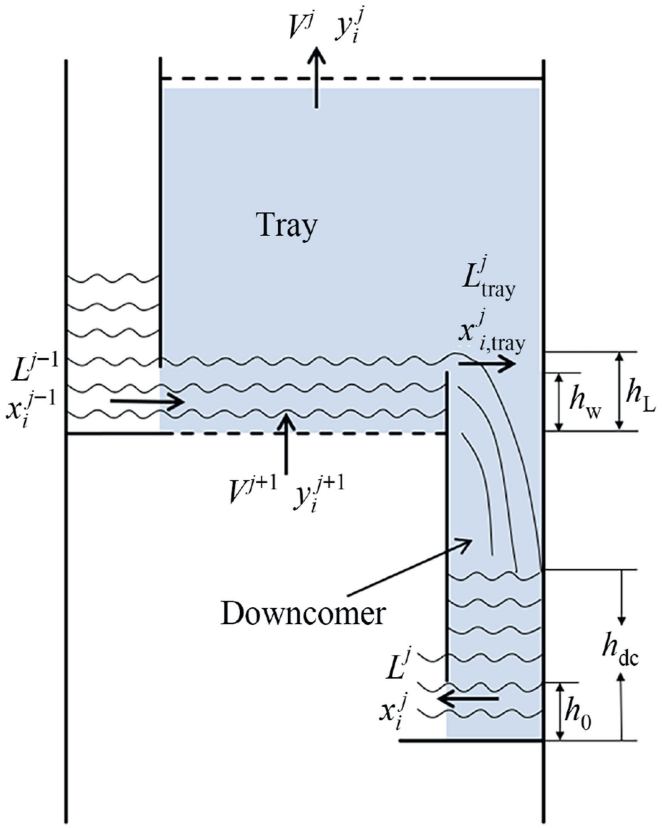

Fig. 1. Schematic diagram of an equilibrium stage j composed of plate tray and downcomer.

influences the hydraulics in the downcomer. All vapor in the downcomer leaves above it and enters the upper tray;

(4) The possible evaporation of the liquid in the downcomer due to reaction heat is ignored.

2.1. Reactive distillation algebrc equation model

The algebraic equilibrium model of RD column stage is presented as follows:

Component mass balance equation of stage j:

For the tray:

$$V^{j+1}y_i^{j+1} + L^{j-1}x_i^{j-1} - V^j y_i^j - L^j_{\text{tray}}x^j_{i,\text{tray}} + R^j_{i,\text{tray}}V^j_{r,\text{tray}} = 0 \quad i = 1,2,\cdots,N_C;\ j = 1,2,\cdots,N_s \tag{1}$$

$$R^j_{i,\text{tray}} = \sum_{k=1}^{Nr} \nu_{i,k} r^j_{k,\text{tray}} \quad i = 1,2,\cdots,N_C;\ j = 1,2,\cdots,N_s;\ k = 1,2,\cdots,N_r \tag{2}$$

$$r^j_{k,\text{tray}} = f\left(T^j, P^j, x^j_{i,\text{tray}}\right) \quad i = 1,2,\cdots,N_C;\ j = 1,2,\cdots,N_s;\ k = 1,2,\cdots,N_r \tag{3}$$

$$V^j_{r,\text{tray}} = (1 - 2f_{da})\frac{\pi}{4}D^2 h^j_l \quad j = 1,2,\cdots,N_s \tag{4}$$

where N_C is the number of components, N_s is the number of stages, N_r is the number of reactions. V^j and L^j_{tray} represent the molar flow rates of vapor and liquid leaving tray j, L^j represents the molar flow rates of liquid phases leaving downcomer j. y_i^j and $x^j_{i,\text{tray}}$ respectively denote the mole fractions of vapor and liquid phases leaving tray j, x_i^j denotes the mole fractions of liquid phases leaving downcomer j. $R^j_{i,\text{tray}}$ denotes the molar reaction rate of component i on tray j. $V^j_{r,\text{tray}}$ denotes the reaction volume on tray j. $\nu_{i,k}$ represents the normalized stoichiometric coefficient of component i in reaction k. $r^j_{k,\text{tray}}$ denotes the molar reaction rate of reaction k on tray j. f_{da} denotes the fractional downcomer area. D represents the column diameter. h_l^j represents the height of the equivalent clear liquid layer on tray j.

For the downcomer:

$$L^j_{\text{tray}}x^j{}_{i,\text{tray}} - L^j x_i^j + R^j_{i,\text{dc}}V^j_{r,\text{dc}} = 0 \quad i = 1,2,\cdots,N_C;\ j = 1,2,\cdots,N_s \tag{5}$$

$$R^j_{i,\text{dc}} = \sum_{k=1}^{Nr} \nu_{i,k} r^j_{k,\text{dc}} \quad i = 1,2,\cdots,N_C;\ j = 1,2,\cdots,N_s;\ k = 1,2,\cdots,N_r \tag{6}$$

$$r^j_{k,\text{dc}} = f\left(T^j_{\text{dc}}, P^j_{\text{dc}}, x_i^j\right) \quad i = 1,2,\cdots,N_C;\ j = 1,2,\cdots,N_s;\ k = 1,2,\cdots,N_r \tag{7}$$

$$V^j_{r,\text{dc}} = f_{da}\frac{\pi}{4}D^2 h^j_{\text{dc}} \quad j = 1,2,\cdots,N_s \tag{8}$$

where $R^j_{i,\text{dc}}$ denotes the molar reaction rate of component i in downcomer j. $V^j_{r,\text{dc}}$ denotes the reaction volume in downcomer j. $r^j_{k,\text{dc}}$ denotes the molar reaction rate of reaction k in downcomer j. h^j_{dc} represents the height of the equivalent clear liquid layer in downcomer j.

Phase equilibrium equation of stage j:

For the tray:

$$y_i^j = K_i^j x^j_{i,\text{tray}} \quad i = 1,2,\cdots,N_C;\ j = 1,2,\cdots,N_s \tag{9}$$

where K_i^j is the phase equilibrium constant of component i on tray j.

For the downcomer:

There is no phase equilibrium equation for the downcomer because according to assumption (3), the vapor entrained by the liquid into the downcomer does not engage in mass transfer with the liquid.

Summation equation of stage j:

For the tray:

$$\sum_{i=1}^{N_c} x^j_{i,tray} = 1, \sum_{i=1}^{N_c} y_i^j = 1 \quad i = 1,2,\cdots,N_C;\ j = 1,2,\cdots,N_s \tag{10}$$

For the downcomer:

$$\sum_{i=1}^{N_c} x_i^j = 1 \quad i = 1,2,\cdots,N_C;\ j = 1,2,\cdots,N_s \tag{11}$$

Heat balance equation of stage j:

For the tray:

$$V^{j+1}h_V^{j+1} + L^{j-1}h_L^{j-1} - V^j h_V^j - L_{tray}^j h_{L,tray}^j = 0 \quad j = 1, 2, \cdots, N_s \tag{12}$$

For the downcomer:

$$L_{tray}^j h_{L,tray}^j - L^j h_L^j = 0 \quad j = 1, 2, \cdots, N_s \tag{13}$$

where h_V^j and $h_{L,tray}^j$ respectively denote the specific enthalpy values of the vapor and liquid streams leaving the tray j. h_L^j denotes the specific enthalpy values of the liquid stream leaving the downcomer j.

2.2. Reaction distillation differential equation model

As mentioned in the first paragraph of Section 2, PT modeling method, which converts algebraic equation model into differential-algebraic equation model, can effectively extend the convergence basin of algebraic equations. Therefore, to deal with the convergence difficulties in solving the RD algebraic equation model, the algebraic component mass balance Eqs. (1) and (5), as well as heat balance Eqs. (12) and (13), which are strong coupled between adjacent stages, are rewritten as differential Eqs. (14), (17), (20), and (22), respectively. In addition, the chemical reactions can lead to the strong nonlinearity of the mass balance equations, therefore the item of $R_i^j V_r^j$ in Eqs. (1) and (5) is modulated by a continuation parameter α^j so that the reaction source item at each stage can be eliminated at the beginning of the integration to stabilize the dynamic model.

Component mass balance equation of stage j:

For the tray:

$$\frac{dM_{i,tray}^j}{dt} = V^{j+1}y_i^{j+1} + L^{j-1}x_i^{j-1} - V^j y_i^j - L_{tray}^j x_{i,tray}^j + \alpha_{tray}^j R_{i,tray}^j V_{r,tray}^j \quad i = 1, 2, \cdots, N_C;\ j = 1, 2, \cdots, N_s \tag{14}$$

$$M_{i,tray}^j = M_{L,tray}^j x_{i,tray}^j + M_V^j y_i^j \quad i = 1, 2, \cdots, N_C;\ j = 1, 2, \cdots, N_s \tag{15}$$

$$\frac{d\alpha_{tray}^j}{dt} = 1 - \alpha_{tray}^j, \alpha_{tray}^j(0) = 0 \quad j = 1, 2, \cdots, N_s \tag{16}$$

For the downcomer:

$$\frac{dM_{i,dc}^j}{dt} = L_{tray}^j x_{i,tray}^j - L^j x_i^j + \alpha_{dc}^j R_{i,dc}^j V_{r,dc}^j \quad i = 1, 2, \cdots, N_C;\ j = 1, 2, \cdots, N_s \tag{17}$$

$$M_{i,dc}^j = M_{L,dc}^j x_i^j \quad i = 1, 2, \cdots, N_C;\ j = 1, 2, \cdots, N_s \tag{18}$$

$$\frac{d\alpha_{dc}^j}{dt} = 1 - \alpha_{dc}^j, \alpha_{dc}^j(0) = 0 \quad j = 1, 2, \cdots, N_s \tag{19}$$

Heat balance equation of stage j:

For the tray:

$$\frac{dH_{tray}^j}{dt} = V^{j+1}h_V^{j+1} + L^{j-1}h_L^{j-1} - V^j h_V^j - L_{tray}^j h_{L,tray}^j \quad i = 1, 2, \cdots, N_C;\ j = 1, 2, \cdots, N_s \tag{20}$$

$$H_{tray}^j = M_{L,tray}^j h_{L,tray}^j + M_V^j h_V^j \quad j = 1, 2, \cdots, N_s \tag{21}$$

For the downcomer:

$$\frac{dH_{dc}^j}{dt} = L_{tray}^j h_{L,tray}^j - L^j h_L^j \quad j = 1, 2, \cdots, N_s \tag{22}$$

$$H_{dc}^j = M_{L,dc}^j h_L^j \quad j = 1, 2, \cdots, N_s \tag{23}$$

where $M_{i,tray}^j$ and $M_{i,dc}^j$ denote the pseudo liquid hold-up of component i on tray j and in the downcomer j, respectively. M_V^j and $M_{L,tray}^j$ represent the pseudo molar hold-up of vapor and liquid phases on tray j, respectively. $M_{L,dc}^j$ represents the pseudo molar hold-up of liquid phases in the downcomer j. H_{tray}^j and H_{dc}^j represent the total enthalpy hold-up on the tray j and in the downcomer j, respectively.

To make the equation squared, simple linear pseudo-transient hold-up correlations proposed by Ma *et al.* [14], as shown in Eq. (24), are adopted to improve the efficiency of the integration process and make the calculation more robust.

$$V = C_V M_V;\ \ L_{tray} = C_{L,tray} M_{L,tray};\ \ L = C_{L,dc} M_{L,dc} \tag{24}$$

Where C_V, $C_{L,tray}$ and $C_{L,dc}$ are constants, generally set to 1800 h^{-1}.

2.3. Hydraulic equation for stage pressure drops

Generally, the stage pressure drop Δp^j for sieve tray column is caused by liquid inventory, h_l, dry tray perforation, h_d, and surface tension, h_σ. The pressure drop correlation of sieve tray proposed by Bennett *et al.* [15] was applied to calculate the three parts of pressure drop in this study.

Pressure drop caused by the height of the clear liquid layer on the tray:

$$h_l = \phi_e \left[h_w + C\left(\frac{Q_l}{l_w \phi_e}\right)^{2/3} \right] \tag{25}$$

where ϕ_e is the effective relative froth density (the ratio of the clear liquid layer height to the foam layer height). h_w is the weir height. Q_l represents the liquid volume flow rate per unit weir length. C is the coefficient related to the weir. l_w is the weir length.

Pressure drop caused by the friction of vapor flow passing through the tray perforations:

$$h_d = \frac{0.499}{c_o^2} \frac{\rho_G U_O^2}{\rho_L g} \tag{26}$$

where c_o is the orifice coefficient, taken as 0.765 in this work. U_O represents the actual vapor velocity based on the hole area.

Pressure drop caused by surface tension:

$$h_\sigma = \frac{6\sigma}{g\rho_L D_H} \tag{27}$$

where σ is the surface tension of the liquid phase. D_H is the hole diameter.

Therefore, the stage pressure drop is calculated by Eq. (28). The reasonable range of stage pressure drop is limited by Eq. (29) [16].

$$\Delta p = \rho_L g(h_l + h_d + h_\sigma) \tag{28}$$

$$0.345\ \text{kPa} \le \Delta p \le 1.03\ \text{kPa} \tag{29}$$

2.4. Hydraulic constraints

(1) Constraint of entrainment flooding

Entrainment flooding represents the operational upper limit of a distillation column, occurring when the internal vapor velocity reaches its maximum value. The entrainment flooding constraint is usually expressed by Eq. (30). The vapor velocity (u_{nf}) based on the net area of the column at flooding point can be determined by the Fair correlation [17] for sieve trays, specifically Eqs. (31)–(33).

$$u_n \le 0.8u_{nf} \tag{30}$$

$$u_{nf} = C_{sbf}\left(\frac{\sigma}{20}\right)^{0.2}\left(\frac{\rho_L - \rho_G}{P_G}\right)^{0.5} \tag{31}$$

$$C_{sbf} = 0.0105 + 8.127\left(10^{-4}\right)\left(H_T^{0.755}\right)\exp\left(-1.463F_{LG}^{0.842}\right) \tag{32}$$

$$F_{LG} = \frac{L}{G}\left(\frac{\rho_G}{\rho_L}\right)^{0.5} \tag{33}$$

where u_n represents the actual operating vapor velocity based on the net area of the column. H_T represents the spacing between trays. G and L respectively stand for the mass flow rates of the vapor and liquid streams.

(2) Weeping constraint

Weeping refers the operational lower limit of a distillation column, occurring when the internal vapor velocity reaches its minimum value. The weeping constraint is usually established by Eq. (34). The minimum superficial liquid velocity based on the hole area, $u_{0,min}$, in Eq. (34) is determined by the empirical weeping correlation proposed by Lockett *et al.* [18], specifically Eq. (35):

$$u_{stage} > u_{0,min} \tag{34}$$

$$\frac{L_P}{A_0} = \frac{0.02}{u_{0,min}\left(\frac{\rho_G}{h_L\rho_L g}\right)^{0.5}} - 0.03 \tag{35}$$

where the maximum weeping amount L_P is typically set as 10% of the normal liquid phase load. u_{stage} represents actual vapor velocity based on hole area. A_0 represents the hole area.

(3) Downcomer constraints

Constraint of downcomer backup flooding:

Downcomer backup flooding [17] means aerated liquid backs up in the downcomer, due to exorbitant pressure drop, liquid height and frictional losses in the downcomer apron. The constraint [19] is expressed by Eq. (36), where the froth height in the downcomer, h'_{dc}, can determined by Eq. (37). Eq. (38) [20] is used to calculate the average froth density in the downcomer, ϕ_{dc}. Eqs. (39)–(42) are used to calculate the clear liquid layer height in the downcomer, h_{dc}.

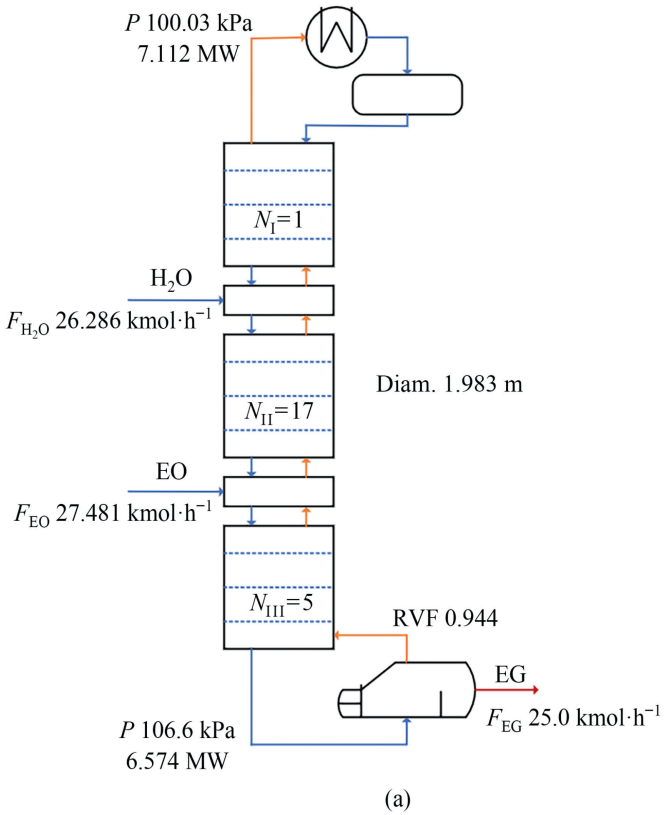

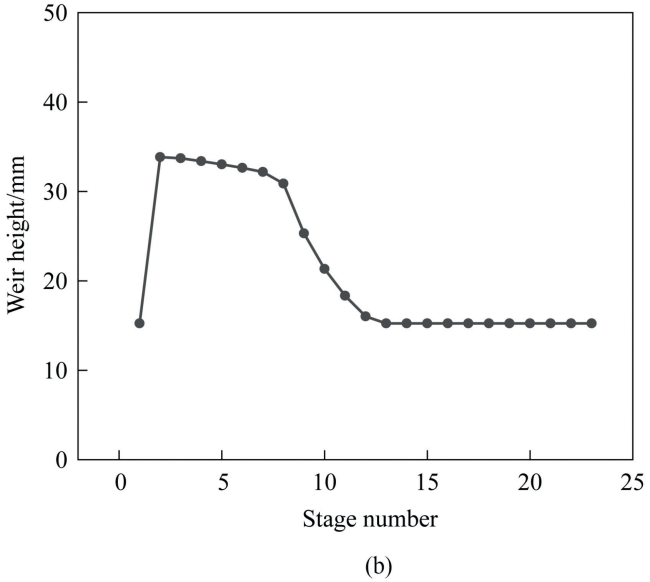

Fig. 2. The result of EG RD column by Li *et al.* [8]: (a) optimal flowsheet results, (b) optimal distribution of weir height.

$$h'_{dc} \le 0.85(H_T + h_w) \tag{36}$$

$$h'_{dc} = \frac{h_{dc}}{\phi_{dc}} \tag{37}$$

$$\phi_{dc} = 0.36617 \frac{0.24215}{1 + \exp\{[378.54 - (\rho_L - \rho_G)]/72.439\}} \tag{38}$$

$$h_{dc} = h_t + h_l + h_{da} \tag{39}$$

$$h_{da} = \frac{0.1652}{0.0254}\left(\frac{Q_{dc}}{A_{da}}\right)^2 \tag{40}$$

$$A_{da} = l_w h_0 \tag{41}$$

$$h_0 = h_w - 0.5 \tag{42}$$

where h_{da} is the head loss under the downcomer apron. Q_{dc} is the liquid volume flow rate in the downcomer. A_{da} represents most restrictive (minimum) area of flow under the downcomer apron, usually, this is the area under the downcomer apron. h_0 is the height of the downcomer clearance. Generally, h_0 should not be less than 0.8–1 in, otherwise the resistance of the liquid through the downcomer clearance will be very high and result in liquid accumulation in the downcomer.

Constraint of downcomer choke flooding:

Downcomer choke flooding may hinder liquid downflow and result in liquid accumulation on the tray above, therefore the liquid velocity at the downcomer entrance, U_{FL}, should be less than the maximum allowable liquid velocity (u_{max}) of the downcomer, as described by Eq. (43). u_{FL} is calculated by Eq. (44).

$$u_{FL} \le u_{max} \tag{43}$$

$$u_{FL} = \frac{Q}{A_{dc}} \tag{44}$$

where Q represents the liquid volume flow rate on the tray.

Downcomer outlet liquid velocity constraint:

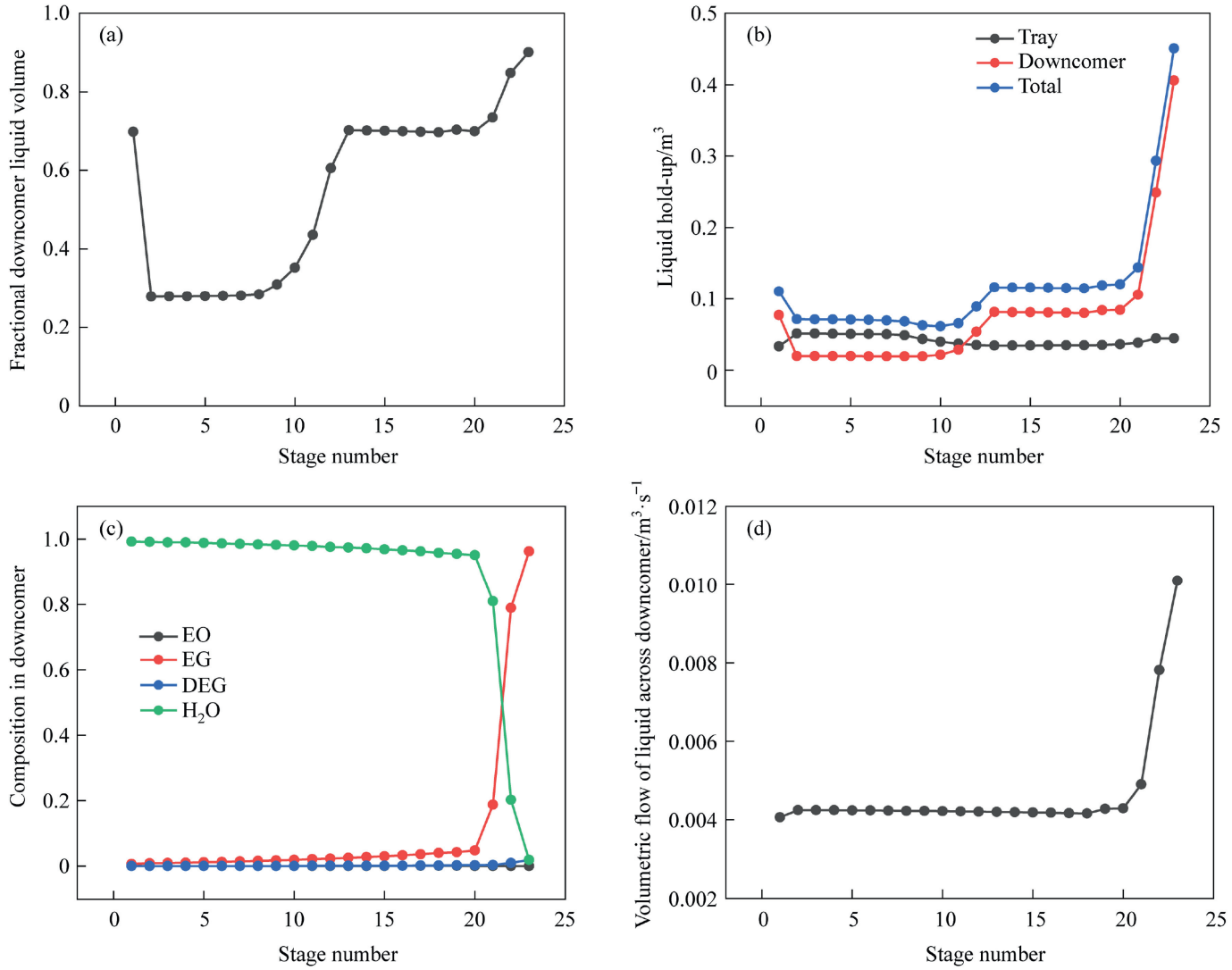

Fig. 3. Evaluated result of (a) fractional downcomer liquid hold-up volume, (b) liquid hold-up distribution between downcomer and tray of each stage, (c) liquid mole fraction of components in downcomer, (d) volumetric flow of liquid across downcomer.

The liquid exiting the downcomer serves as a pre-distribution before entering the next stage, affecting the flow pattern of the liquid on the tray. Therefore, it is essential to maintain the outlet liquid velocity u_{dc} of the downcomer within a reasonable range. In addition, reasonable downcomer outlet liquid velocity also ensures that the downcomer clearance height is not too low. In this work, $u_{dc,max}$ was taken as 0.56 m·s^{-1}. The constraint is expressed by Eq. (45), where outlet liquid velocity of the downcomer, u_{dc}, is calculated by Eq. (46).

$$u_{dc} \leq u_{dc,max} \tag{45}$$

$$u_{dc} = \frac{Q_{dc}}{A_{da}} \tag{46}$$

2.5. Bypass efficiency for stage number optimization

In order to optimize the number of stages of the RD column, the bypass efficiency method proposed by Dowling and Biegler [21] was adopted, which by assigning a continuous bypass efficiency ε^j to each stage, the integer value (0 or 1) of each stage can be obtained at the optima. Then the total number of stages is calculated by Eq. (47):

$$N_{stage} = \sum_{j=1}^{N_s} \varepsilon^j \tag{47}$$

Correspondingly, the pressure on stage j is defined as:

$$P^{j+1} = P^j + \varepsilon^j \Delta p^j \tag{48}$$

where pressure drop Δp^j on tray j is determined by Eq. (28).

2.6. Objective function

The objective of RD column optimization in this study was the minimum annual total cost (TAC), which is the summation of equipment cost and energy cost [22]. Equipment cost includes column equipment cost $C_{col,cap}$ and heat exchanger equipment cost $C_{hx,cap}$. The specific TAC calculation model is as follows:

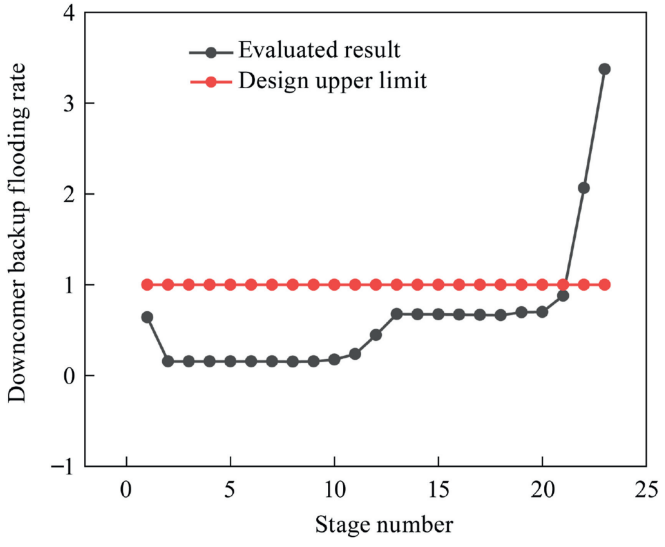

Fig. 4. Situation of downcomer backup flooding rate in the RD column of Li *et al.* [8].

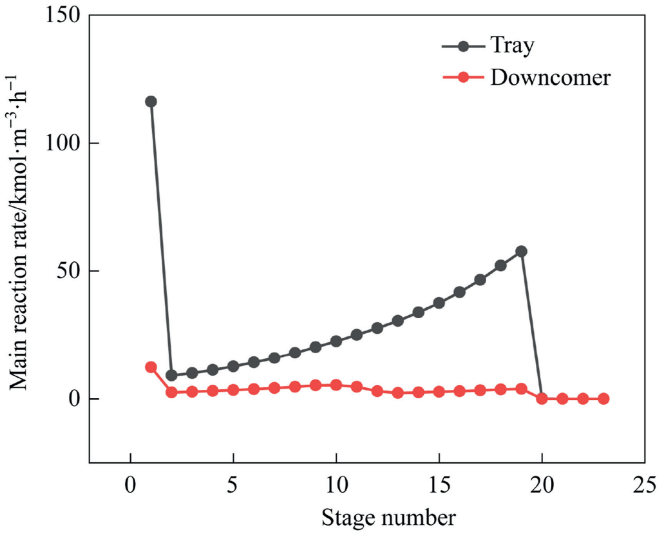

Fig. 5. Evaluated result of main reaction rate.

$$\text{TAC} = \left(C_{col,cap} + C_{hx,cap}\right) \Big/ (\text{Payback period}) + C_{energy} \tag{49}$$

Detail TAC formulas were listed in Appendix A and B for different case study examples.

So far, the PT RD column model considering liquid hold-up in downcomers and tray hydraulics has been formulated. In order to simultaneously optimize operating variables (continuous variables) and structure variables (discrete variables) of the RD column by gradient-based optimization algorithm in EO environment, the

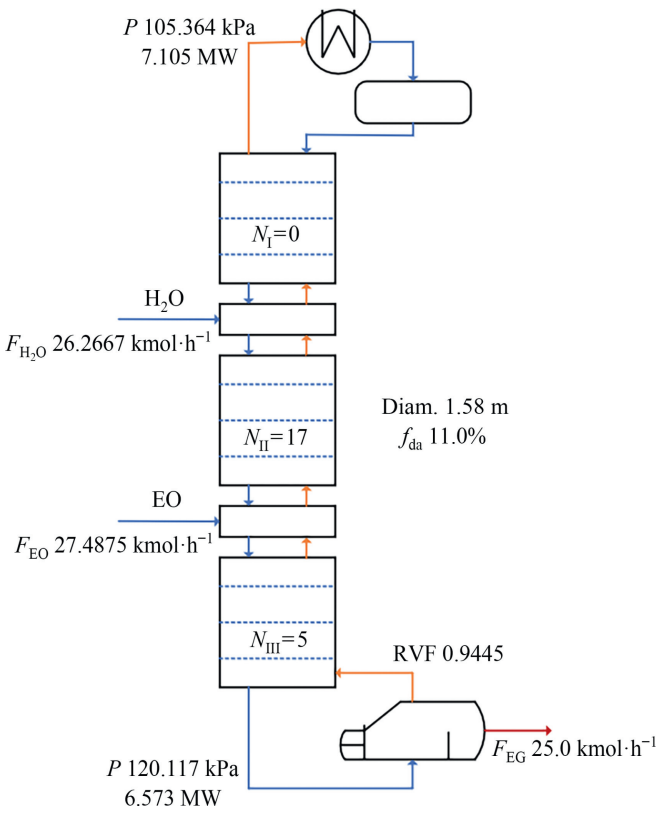

Fig. 6. The optimal result of EG RD column using present model.

Table 1
Weir height in each column section of EG RD column

Column section	I	II	III
Weir height (h_w)/mm	–	68.58	42.42

steady-state optimization algorithm assisted by the PT model proposed by Ma *et al.* [23] was adopted, in which the inner loop conducts steady-state optimization based on an algebraic model, if the steady-state optimization fails, then goes to the outer loop where the pseudo-transient simulation using PT model is performed to converge the current trial point followed by next steady-state optimization.

3. Case Study

In this section, two RD cases in literatures were studied to explore and verify the impact of liquid hold-up in downcomers on the design of RD columns. Each case was firstly evaluated using the proposed model in this study to show whether the column operated normally under the original design parameters obtained by the literature. Subsequently, the column was optimized with the objective of minimum TAC based on the proposed model. In the two cases, distillation columns are all sieve-tray columns, with the sieve tray hole diameter 0.00476 m.

3.1. Ethylene glycol (EG) RD column

The hydration of ethylene oxide (EO) to ethylene glycol (EG) is an irreversible sequence of reaction. EO reacts with water to form EG, however, EG can further reacts with EO to form diethylene glycol (DEG), DEG further reacts with EO to form triethylene glycol, and so on, which may lead to the formation of high molecular weight polymers. The RD process with total reflux operation for producing EG can achieve a lower molar ratio of water to EO in the feed, significantly reducing energy consumption, enhancing product selectivity, and minimizing by-product formation, because the simultaneous separation of components during the RD process can inhibit the side reactions, only the first two reactions usually occur in the RD column:

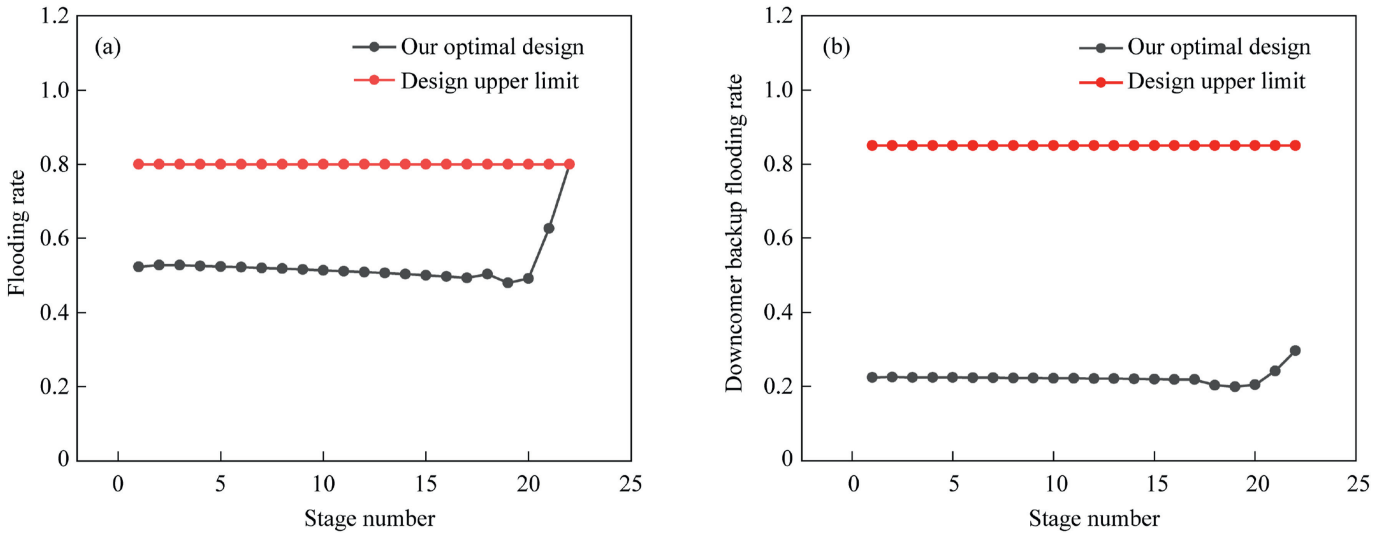

Fig. 7. Optimal result of (a) flooding rate, (b) downcomer backup flooding rate.

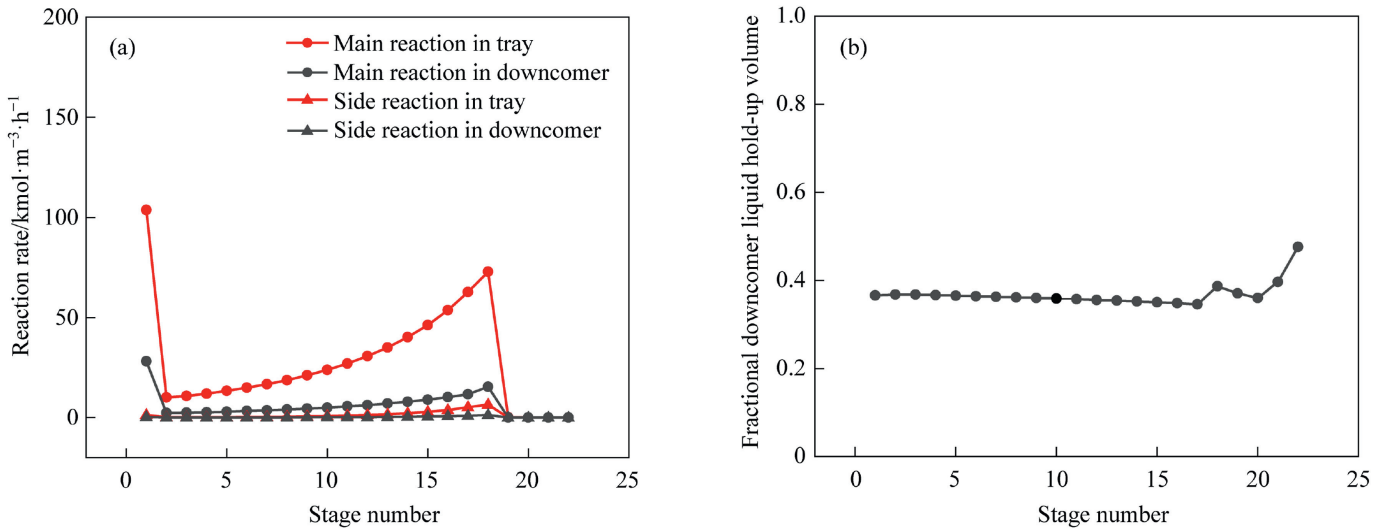

Fig. 8. Optimal result of (a) reaction rate, (b) fractional downcomer liquid hold-up volume.

$$C_2H_4O + H_2O \rightarrow C_2H_6O_2 \quad (50)$$

$$C_2H_4O + C_2H_6O_2 \rightarrow C_4H_{10}O_3 \quad (51)$$

The reaction kinetics equations were from Ciric and Gu [24], as shown in Eqs. (52) and (53). The Wilson equation of state was used as the thermodynamic model. The unit of reaction rate is $mol \cdot cm^{-3} \cdot s^{-1}$.

$$r_1 = 3.15 \times 10^9 \exp(-9547 / T) x_{C_2H_4O} x_{H_2O} \quad (52)$$

$$r_2 = 6.3 \times 10^9 \exp(-9547 / T) x_{C_2H_4O} x_{C_2H_6O_2} \quad (53)$$

This RD column processes EO and water as separate feeds, with pressures and vapor fraction being 121.59 kPa and 0, respectively. The requirement of EG yield in the bottom stream was not less than 25 $kmol \cdot h^{-1}$.

To simplify the RD model and make it easy to solve, Li *et al.* [8] assumed that all the liquid hold-up of a stage belongs to the tray, Fig. 2 shows the results of the EG RD column optimized by Li *et al.* To evaluate the performance of Li *et al.*'s column, we simulated the column using the proposed model in this study, which considered the liquid hold-up of a tray and its downcomer separately, based on the operational conditions and equipment parameters obtained by Li *et al.*

Fig. 3 shows the evaluated results of Li *et al.*'s design using the present model. Li *et al.* assumed all the liquid hold-up of a stage belonging to the tray, however, as shown in Fig. 3(a), the liquid hold-up in a downcomer accounted for more than 30% of the liquid hold-up at the stage. Therefore, the column diameter was overestimated by Li *et al.* because they calculated the column diameter using the optimized reaction volume without subtracting the volume of liquid hold-up in the downcomer. Moreover, the downcomer liquid hold-up accounted for a large proportion in stage 1 and stages 13–23. In the design of Li *et al.*, according to Eq. (42) (the unit used in the equation is in), the weir height of stage 1 and stages 13–23 was 15.24 mm, therefore the downcomer clearance height was only 2.54 mm, excessive resistance caused a larger amount of liquid hold-up in the downcomer, as shown in Fig. 3(b). At stages 22 and 23, the fractional downcomer liquid hold-up volume was particularly high, which was mainly caused by the changes in the composition of the liquid phase in the column. It could be seen from the liquid composition of the components in each stage downcomer in Fig. 3(c) that stages 22 and 23 mainly played a role in separation. In stages 1–20, the main component was water, while in stages 22 and 23, the main component was EG. Due to the decrease of the water at the bottom of the column and the increase of EG, the liquid molar density at the bottom of the column was greatly reduced. The liquid volume flow rate increased significantly in stages 22 and 23, as shown in Fig. 3(d). As a result, the resistance of the liquid through the downcomer clearance increased further and the liquid hold-up in downcomer increases again. Therefore, severe downcomer backup flooding occurred at stages 22 and 23 in Li *et al.*'s design, as shown in Fig. 4.

In addition, assuming that the liquid hold-up of a stage belongs to its tray, it is equivalent to assuming that the reaction rate on the tray is the same as the reaction rate in the downcomer. However, the evaluated results of main reaction rate distribution in Fig. 5 showed that the reaction rate on the tray was much higher than that in the downcomer. Therefore, ignoring the difference in reaction rate between the liquid phase on the tray and the liquid phase in the downcomer would also lead to the design deviation of the RD column structural parameters.

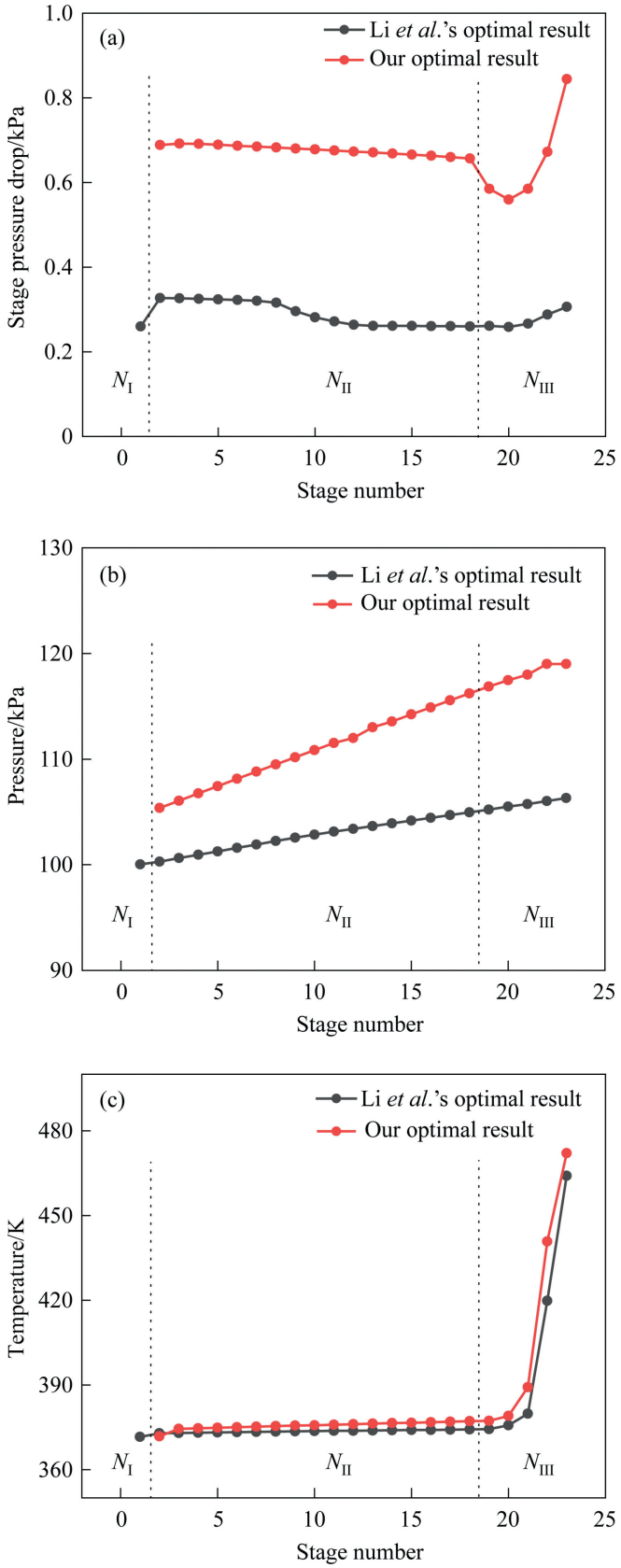

Fig. 9. Optimal results comparison of Li *et al.* and present model: (a) pressure drop of stages, (b) pressure, (c) temperature.

To achieve accurate design of the EG RD column, we optimized the column using the proposed RD model considering the reactions in the liquid hold-ups on column trays and in downcomers, stage pressure drop, and column hydraulics constraints. And to address the issue of excessive model complexity and computational difficulties, a steady-state optimization method assisted by the PT model was used to simultaneously optimize discrete variables of column structure and continuous operating variables. The optimization variables selected in this example were the column diameter, the number of trays, the uniform weir heights of each column section, the column top pressure, the molar flow rate of glycol and water, the vapor fraction of reboiler (RVF), and the additional fractional downcomer area. The fractional hole area was 12%.

Fig. 6 and Table 1 show the optimized results of the EG RD column. Notably, compared with the results of Li *et al.*, the number of stages in section II and III has not changed, while the number of stages in section I changes from 1 to 0, implying water is fed from the top of the column. The optimal column diameter is 1.58 m, which is significantly smaller than 1.983 m by Li *et al.*, therefore the liquid flooding rate of each tray tend to its upper limit within the feasible range, as shown in Fig. 7(a). The optimal weir heights for the column section II and III are higher than those in Li *et al.*'s design, thus the height of downcomer clearances increase significantly and downcomer backup flooding is eliminated, as shown in Fig. 7(b).

Fig. 8(a) shows the distribution the main and side reaction rates in the EG RD column, no matter on the tray or in the downcomer, the reaction section is stage 1–19, and almost no reaction occurs in the last four stages. Fig. 8(b) is the distribution of fractional downcomer liquid hold-up in the EG RD column.

Fig. 9 illustrates the distribution of stage pressure drop, pressure, and temperature in the column. The bottom pressure obtained in this design is 119.3 kPa, higher than the 106.6 kPa in Li *et al.*'s design. This is because the weir height optimized in this study is higher than that in Li *et al.*'s design, resulting in a higher clear liquid layer height on the tray. Additionally, due to the smaller column diameter, the apparent vapor velocity in the column is higher, leading to a higher hole velocity and consequently, a greater dry tray resistance. Therefore, the larger clear liquid layer height on the tray and the dry tray resistance result in a higher tray pressure drop than that in Li *et al.*'s design, as shown in Fig. 9(a). The bottom temperature (472.1 K) is also higher than Li *et al.*'s temperature (464.1 K).

According to the optimization results of this example case, the liquid hold-up in downcomers not only affect the RD column structural variables such as column diameter and weir height, but also affects the distribution of pressure drop and temperature in the column, thereby the conditions of the reaction kinetics and phase equilibrium. Therefore, it is essential to consider the downcomer liquid hold-up to ensure a more accurate design of the RD column.

3.2. Methyl acetate (MeOAc) RD column

To further verify the impact of downcomer liquid hold-up on the design and operation of RD columns, a methyl acetate RD column designed by Li *et al.* [8] was simulated and optimized in this section. Methyl acetate is produced by esterification of acetic acid and methanol, as described by Eq. (54), which is a reversible reaction under heterogeneous catalyst.

$$\mathrm{HOAc} + \mathrm{MeOH} \rightleftharpoons \mathrm{MeOAc} + \mathrm{H_2O} \tag{54}$$

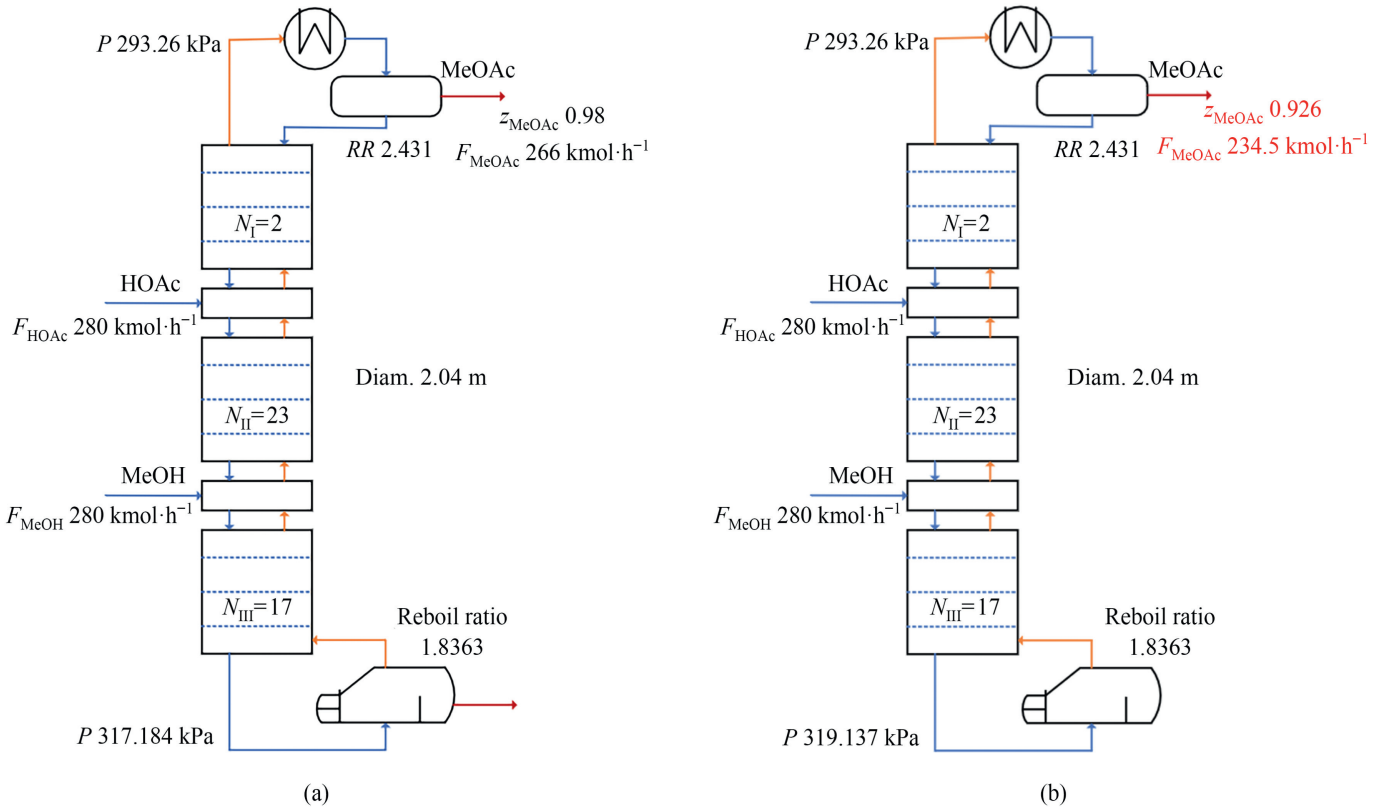

Fig. 10. Results comparison: (a) the result of Li *et al.*; (b) the evaluated result by the proposed model in this study.

The activity-based reaction rate model based on pseudo-homogeneous reaction assumption is as follows:

$$r = k_f \left(a_{HOAc} a_{MeOH} - \frac{a_{MeOAc} a_{H_2O}}{K_{eq}} \right) \tag{55}$$

where the reaction equilibrium constant K_{eq}, and the forward rate constant k_f [25] are given by Eqs. (56) and (57).

$$K_{eq} = 2.32 \exp\left(\frac{782.98}{T}\right) \tag{56}$$

$$k_f = 9.732 \times 10^8 \exp\left(-\frac{6287.7}{T}\right) \tag{57}$$

For catalysts in the heterogeneous RD plate column, there are three common internal configurations: vertically disposed catalyst-containing envelopes placed along the direction of the liquid flow path across a tray, within downcomers or near the exit of the downcomers, and catalytic plates and separation plates installed alternately. The first type of configuration [26,27] ensures good contact between the liquid and the catalyst without excessive pressure drop. The primary drawback of the second type [26,28] is the limited volume available for catalyst inventory, and the gas phase barely passes through the catalyst, resulting in poor separation performance in the reaction zones. The third type [29] can address both reaction and separation performance but at the cost of an increased number of trays and column pressure drop. Because it is relatively convenient to obtain the hydraulic parameters for the first type of configuration, this paper performed rigorous simulation and optimization only for the RD column with catalysts placed on trays. However, the method proposed in this study is also applicable for the last two types of configurations, given the hydraulic parameters for specific catalyst internals. Although there is no reaction in the downcomer in the first type of configuration, the liquid hold-up in the downcomer will also affect the hydraulic limitation of the downcomer, thus affecting the normal operation of the column.

Acetic acid and methanol are fed with equal molar flow rates of 280 kmol·h^{-1}, with a pressure and vapor fraction of 405.3 kPa and 0, respectively. The purity of MeOAc in distillate should not be less than 98% (mass), and the conversion rate of the reactants should not be less than 95% (meaning the MeOAc flow at the top of the column should be no less than 266 kmol·h^{-1}).

Because Li *et al.* assumed that all the liquid hold-up of a stage belonged to the tray, only the tray hydraulics were considered in their design, and the downcomer hydraulics were ignored. Li *et al.* optimized the RD column with liquid hold-up as an optimization variable, and for simplification, they calculated the liquid hold-up by Eq. (58), where A_T is total column cross-section area. However, in real plate column, the effective zone of a tray is bubbling area, and the height of clear liquid is approximately 10%–40% of the weir height [17]. There no doubt, the liquid hold-up calculated by Li *et al.* is obviously overestimated. Additionally, Li *et al.* did not consider the liquid hold-up and the hydraulics in the downcomer of the column, which may lead to the hydraulics infeasibility.

$$V_r^j = A_T h_w^j \tag{58}$$

Fig. 10 shows the design by Li *et al.* (Fig. 10(a)) and the evaluation result by the model proposed in this study (Fig. 10(b)). It is found that the purity of MeOAc in distillate is 0.926, and the flow of MeOAc is 234.5 kmol·h^{-1}, which cannot meet the requirements.

Fig. 11 shows the hydraulic conditions of the MeOAc RD column evaluated by the model proposed in this study. Fig. 11(a) reveals the weeping on the stages 20–42 owing to the excessively low vapor

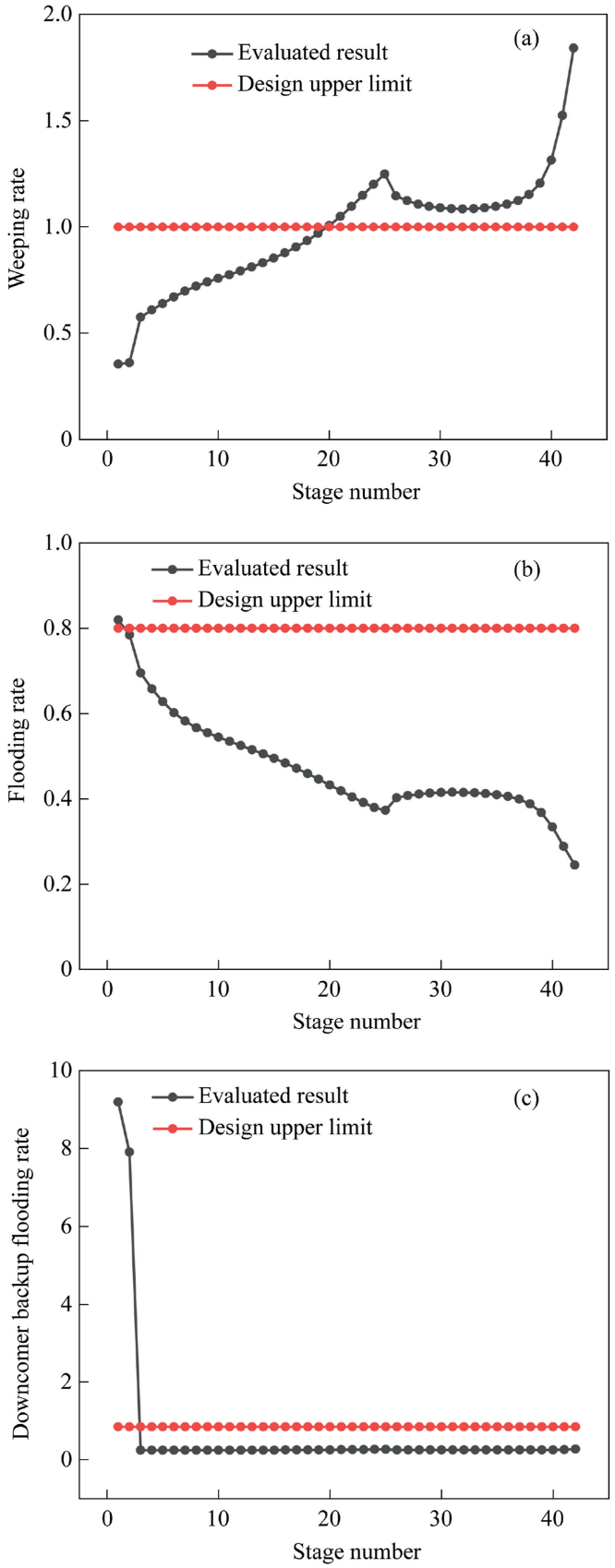

Fig. 11. Distribution of (a) weeping rate, (b) flooding rate, (c) downcomer backup flooding rate.

Table 2
Comparison of weir height, column diameter and the number of trays in each column section of the optimal MeOAc RD column

Column section		I	II	III
Weir height (h_w)/mm	Li *et al.*	15.24	127.00	92.46
	This study	50.8	82.4	134.3
Column diameter (D)/m	Li *et al.*	2.04		
	This study	2.36	2.48	1.74
The number of trays	Li *et al.*	2	23	17
	This study	5	38	17

velocity in corresponding stages, in fact, the low flooding rate at the bottom of the column in Fig. 11(b) confirms the low vapor rate. The small weir height of column section I designed by Li *et al.*, as shown in Table 2, which may lead to a small height of the downcomer clearance, resulting a significant resistance when liquid passes through the downcomer outlet in column section I. Therefore, severe downcomer backup flooding occurred in the first two stages of the column, as shown in Fig. 11(c).

To obtain an accurate design, the MeOAc RD column was optimized based on the proposed RD model. The optimization variables of this case were the column diameter and number of trays for each column section, weir height of column section II and III, the column top pressure, the reflux ratio, the reboiling ratio, and fractional downcomer area. And the fractional downcomer area was considered as an additional optimization variable. Note that, to avoid the weeping owing to small gas velocity in the column bottom, a small fractional hole area of 8% was adopted in this case, and since there was almost no reaction in column section I and no catalyst installed, this section was a conventional rectifying section without reaction. In contrast, column section II and III were the reaction sections. The weir height of column section I was not optimized and was fixed at 50.8 mm because there was no additional requirement for liquid hold-up in conventional distillation. The optimization results were shown in Fig. 12 and Table 2.

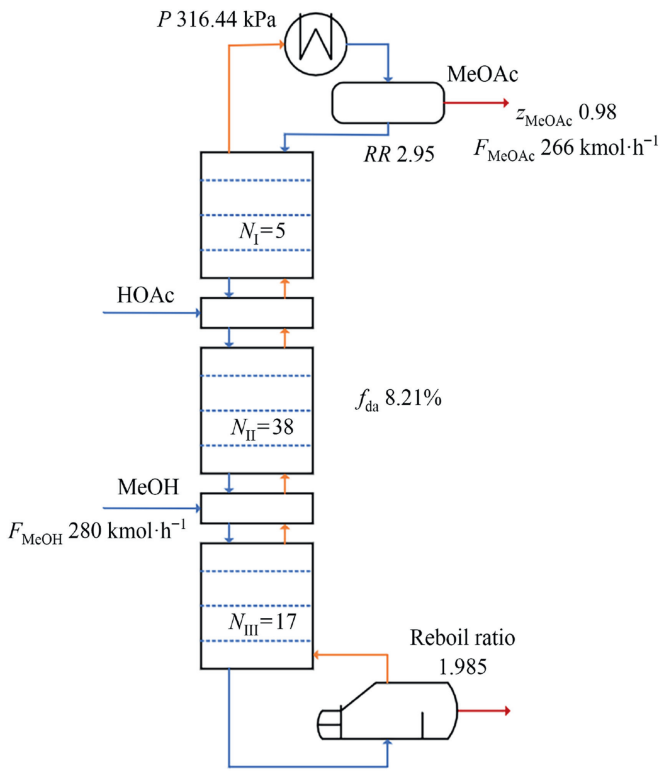

Fig. 12. Flowsheet results of the optimal MeOAc RD column.

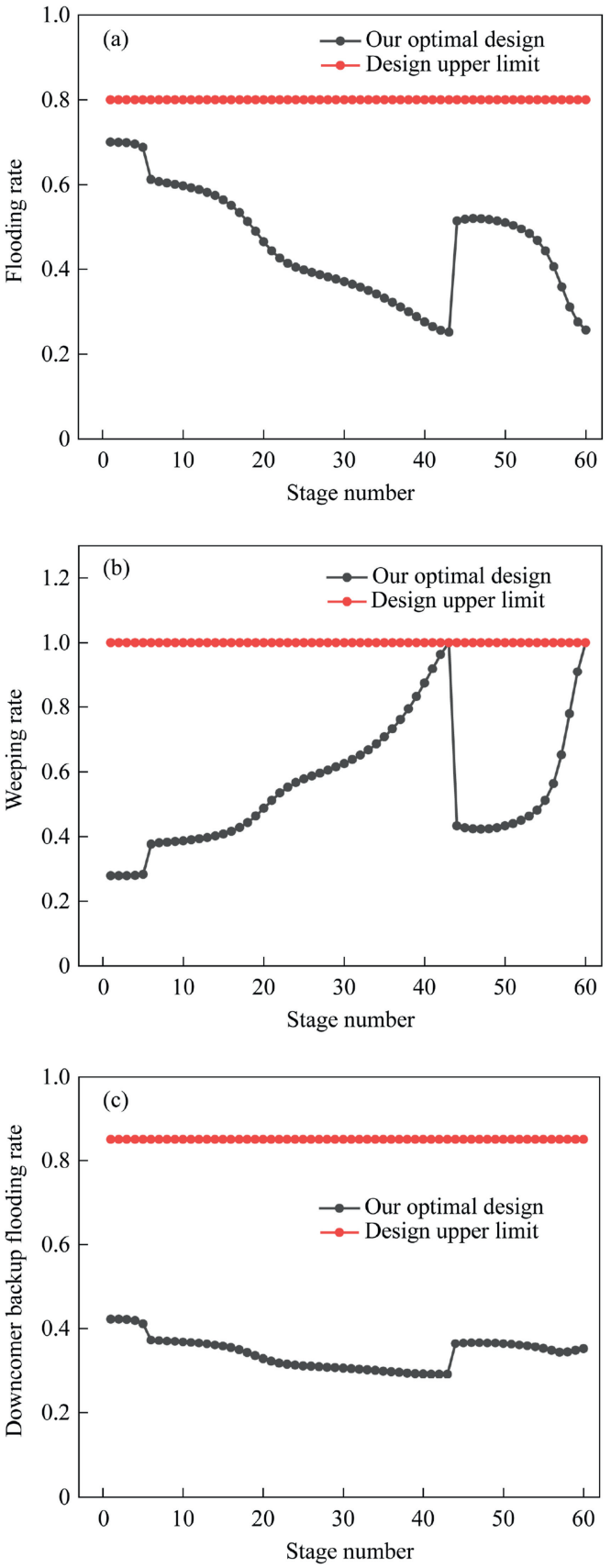

Fig. 13. Distribution of (a) flooding rate, (b) weeping rate, (c) downcomer backup flooding rate.

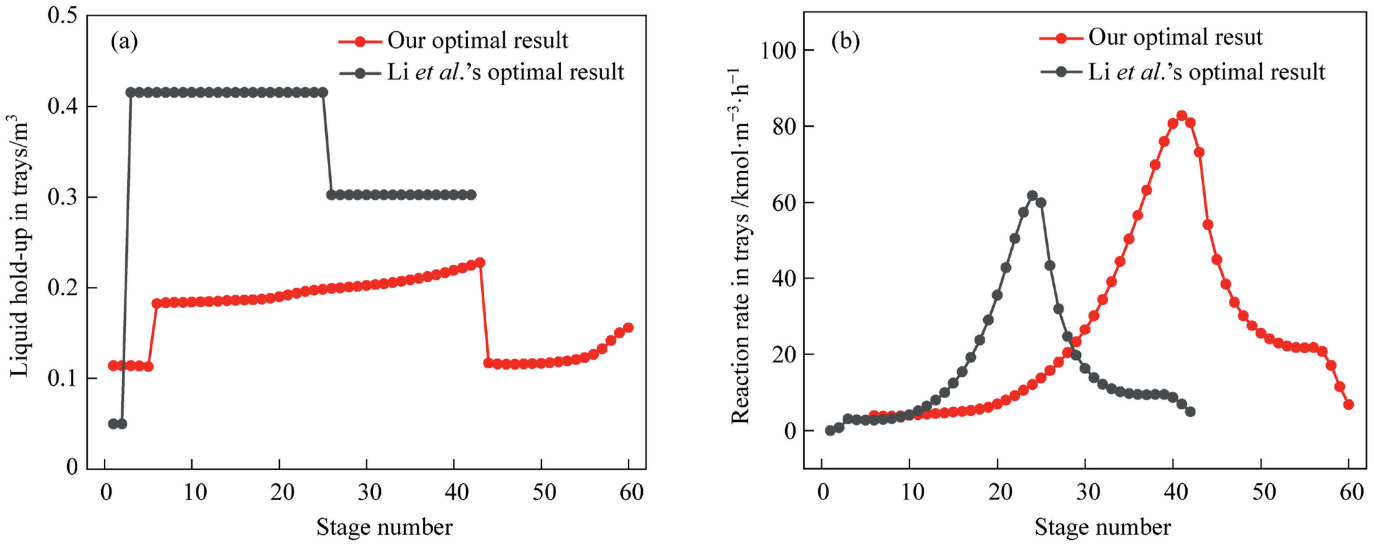

Fig. 14. Comparison of optimal results of liquid hold-up and reaction rate in trays: (a) liquid hold-up in trays, (b) reaction rate in trays.

From the optimization results, it's evident that the column diameter, weir height, and the number of trays significantly changed when the downcomer liquid hold-up was considered. According to the new design, there was no flooding occurred in the column, as shown in Fig. 13(a). The lowest gas velocity reached at the last stage of the column section II and III, so the weeping there reached their upper limit, as shown in Fig. 13(b). The downcomer backup flooding met the constraints because of adequate wire high optimized, as shown in Fig. 13 (c).

When the liquid hold-up without reaction in the downcomer was taken into account, compared with the design by Li *et al.*, the number of trays increased while the liquid hold-up of each tray decreased, as shown in Fig. 14 (a). At the same time, there was an increase in optimized operating pressure (335.14 kPa), resulting in an increase in the temperature in the column, and the reaction rate on each tray also increased, as shown in Fig. 14 (b), which is also one of the reasons why the weir height required in the reaction section is smaller than the design by Li *et al.*

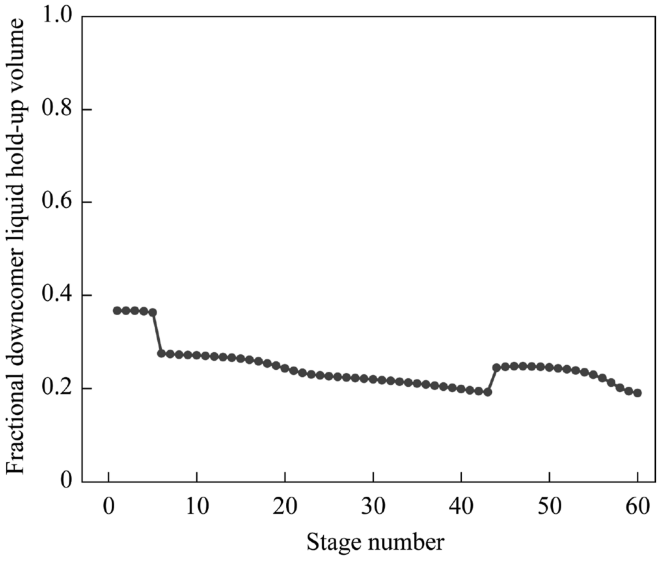

Fig. 15. Distribution of fractional downcomer liquid hold-up volume.

The optimal fractional downcomer liquid hold-up volume in a homogeneous RD column is a trade-off of the liquid hold-up and the extent of reaction in the tray and downcomer to achieve the minimum TAC. For this MeOAc RD column, as there was no catalyst in the downcomer, the optimized downcomer liquid hold-up proportion in the total liquid hold-up at all stages (as shown in Fig. 15) was reduced compared to Case 1, so as to ensure that there was sufficient liquid hold-up on trays for adequate reaction.

4. Conclusions

In this study, a rigorous pseudo-transient equilibrium RD model that considers liquid hold-up on trays and in downcomers, as well as the column hydraulic, was developed to assess their effects on reaction, separation and operation in an RD plate column. A steady-state optimization algorithm assisted by the pseudo-transient RD model was used to simultaneously optimize both structural and operational variables. The influence of liquid hold-up in both downcomers and column trays on the operation and optimization design of RD columns was explored, and rigorous simulation and optimization design of RD columns were realized.

The evaluation and optimization study of the EG homogeneous RD column revealed that assuming all liquid hold-up of a stage is solely attributed to the tray tends to overestimate the tray's liquid hold-up and ignores the differences in reaction rates between the tray and the downcomer. This results in significant deviations in the optimized liquid hold-up. Additionally, the study of the MeOAc heterogeneous RD column demonstrated that neglecting the liquid hold-up in the downcomer leads to an inaccurate design of the downcomer structural parameters, which may render the downcomer hydraulically infeasible and potentially affect the optimization results for the tray parameters, thereby impacting the optimized liquid hold-up design. Furthermore, the pressure drop of each tray, as well as the pressure and temperature distribution in the column, were significantly affected by the liquid hold-up in the downcomers. This further altered reaction kinetics and phase equilibrium conditions, causing substantial deviations in the optimized column diameter, weir height, and number of trays.

This study proves that attributing all liquid hold-up of a stage to the tray leads to significant deviations from the actual situation and may render the designed column operationally

infeasible. Therefore, it is crucial to accurately calculate the downcomer liquid hold-up. The model proposed in this study accurately computes the liquid hold-up in both trays and downcomers separately and facilitates robust optimization using the steady-state optimization method assisted by the PT model. This study provides guidance for achieving more accurate and operable optimization design of RD plate columns. However, it does not account for the mass transfer between the vapor and liquid entering the downcomer, which may affect the optimal design. Future research should consider mass transfer in downcomers to achieve more precise designs.

CRediT Authorship Contribution Statement

Du Yuchang: Writing – original draft, Methodology, Formal analysis, Data curation, Conceptualization. Luo Yiqing: Writing – review & editing, Supervision, Conceptualization. Yang Peilin: Writing – review & editing, Conceptualization. Jia Shengkun: Supervision. Yuan Xigang: Supervision.

Declaration of Competing Interest

The authors declare that they have no known competing financial interests or personal relationships that could have appeared to influence the work reported in this paper.

Acknowledgements

This study was supported by the National Natural Science Foundation of China (22378304).

Nomenclature

A_{da}	the area under the downcomer apron, m^2
A_0	hole area, m^2
C_V, $C_{L,tray}$, $C_{L,dc}$	pseudo-liquid hold-up constant, h^{-1}
f_{da}	fractional downcomer area
h_{da}	the head loss under the downcomer apron, in
h_{dc}	the clear liquid layer height in the downcomer, in
h'_{dc}	the froth height in the downcomer, in
h_l	the height of the equivalent clear liquid layer height, in
h_w	weir height, in
h_0	the height of the downcomer clearance, in
K_i^j	the phase equilibrium constant of component i on tray j
k_f	the forward rate constant, h^{-1}
L^j	molar flow rates of the liquid phase entering tray j, $kg\cdot m^{-3}\cdot s^{-1}$
L^j_{tray}	the molar flow rates of liquid phases leaving tray j, $kmol\cdot h^{-1}$
l_w	weir length, in
M_i^j	molar hold-ups of component i on stage j, kmol
M_L^j	molar hold-ups of liquid phases on stage j, kmol
M_V^j	molar hold-ups of vapor phases on stage j, kmol
Q_{dc}	the liquid volume flow rate in the downcomer, $m^3\cdot s^{-1}$
Q_l	the liquid flow rate, $gal\cdot min^{-1}$ (1 gas=0.00379 m^3)
R_i^j	the molar reaction rate of component i on stage j, $kmol\cdot m^{-3}\cdot h^{-1}$
RR	reflux ratio
RVF	vapor fraction of the reboiler
r_k^j	the molar reaction rate of reaction k on stage j, $kmol\cdot m^{-3}\cdot h^{-1}$
T	temperature, K
U_O	actual vapor velocity based on the hole area, $ft\cdot s^{-1}$
u_{dc}	the maximum clear liquid velocity at the downcomer outlet, $m\cdot s^{-1}$
u_{FL}	the maximum clear liquid velocity at the downcomer entrance, $m\cdot s^{-1}$
u_n	actual gas velocity based on the net area of the column, $m\cdot s^{-1}$
u_{nf}	vapor velocity based on the net area of the column during flooding, $m\cdot s^{-1}$
$u_{0,min}$	lower limit of the steam velocity based on the hole area, $m\cdot s^{-1}$
V^j	the molar flow rates of vapor phases leaving tray j, $kmol\cdot h^{-1}$
$V^j_{r,dc}$	the reaction volume in downcomer j, m^3
$V^j_{r,tray}$	the reaction volume on tray j, m^3
$\nu_{i,k}$	normalized stoichiometric coefficient of component i in reaction k
α	integrated parameter
ρ_G	density of vapor, $kg\cdot m^{-3}$
ρ_L	density of liquid, $kg\cdot m^{-3}$
σ	surface tension, $dynes\cdot cm^{-1}$
ϕ_e	effective relative froth density

References

[1] A.A. Kiss, R. Smith, Rethinking energy use in distillation processes for a more sustainable chemical industry, *Energy* 203 (2020) 117788.
[2] Z.Y. Kong, E. Sánchez-Ramírez, A. Yang, W.F. Shen, J.G. Segovia-Hernández, J. Sunarso, Process intensification from conventional to advanced distillations: past, present, and future, *Chem. Eng. Res. Des.* 188 (2022) 378–392.
[3] A.A. Kiss, M. Jobson, X. Gao, Reactive distillation: stepping up to the next level of process intensification, *Ind. Eng. Chem. Res.* 58 (2019) 5909–5918.
[4] R.S. Huss, F.R. Chen, M.F. Malone, M.F. Doherty, Reactive distillation for methyl acetate production, *Comput. Chem. Eng.* 27 (12) (2003) 1855–1866.
[5] W.L. Luyben, K.M. Pszalgowski, M.R. Schaefer, C. Siddons, Design and control of conventional and reactive distillation processes for the production of butyl acetate, *Ind. Eng. Chem. Res.* 43 (25) (2004) 8014–8025.
[6] A. Harwardt, K. Kraemer, B. Rüngeler, W. Marquardt, Conceptual design of a butyl-levulinate reactive distillation process by incremental refinement, *Chin. J. Chem. Eng.* 19 (3) (2011) 371–379.
[7] A. Tsatse, S.R.G. Oudenhoven, A.J.B. ten Kate, E. Sorensen, Optimal design and operation of reactive distillation systems based on a superstructure methodology, *Chem. Eng. Res. Des.* 170 (2021) 107–133.
[8] K.Y. Li, Y.Q. Luo, X.G. Yuan, Equation-oriented optimization of reaction distillation column considering tray hydraulics, *Sep. Purif. Technol.* 295 (2022) 121229.
[9] L. Domingues, C.I.C. Pinheiro, N.M.C. Oliveira, Optimal design of reactive distillation systems: application to the production of ethyl tert-butyl ether (ETBE), *Comput. Chem. Eng.* 64 (2014) 81–94.
[10] J.G. Segovia-Hernández, S. Hernández, A. Bonilla Petriciolet, Reactive distillation: a review of optimal design using deterministic and stochastic techniques, *Chem. Eng. Process. Process. Intensif.* 97 (2015) 134–143.
[11] Y.J. Ma, Y.Q. Luo, X.G. Yuan, Equation-oriented optimization of reactive distillation systems using pseudo-transient models, *Chem. Eng. Sci.* 195 (2019) 381–398.
[12] L. Noll, L. van der Ham, S. Oudenhoven, A. ten Kate, G. Bargeman, S. Kersten, Extension of the equilibrium stage model to include rigorous liquid holdup calculations for reactive distillation, *Processes* 11 (4) (2023) 1131.
[13] R.C. Pattison, M. Baldea, Equation-oriented flowsheet simulation and optimization using pseudo-transient models, *AIChE J.* 60 (12) (2014) 4104–4123.
[14] Y.J. Ma, Y.Q. Luo, X.G. Yuan, Simultaneous optimization of complex distillation systems with a new pseudo-transient continuation model, *Ind. Eng. Chem. Res.* 56 (21) (2017) 6266–6274.
[15] D.L. Bennett, R. Agrawal, P.J. Cook, New pressure drop correlation for sieve tray distillation columns, *AIChE J.* 29 (3) (1983) 434–442.
[16] J.D. Seader, E.J. Henley, D.K. Roper, Separation Process Principles, third ed., John Wiley Incorporated, Hoboken, NJ, USA, 2010.
[17] D.W. Green, M.Z. Southard (Eds.), Perry's Chemical Engineers' Handbook, ninth ed., McGraw Hill Education, New York, NY, USA, 2019.
[18] M.J. Lockett, S. Banik, Weeping from sieve trays, *Ind. Eng. Chem. Process Des. Dev.* 25 (2) (1986) 561–569.
[19] V.M. Enríquez-Gutiérrez, M. Jobson, L.M. Ochoa-Estopier, R. Smith, Retrofit of heat-integrated crude oil distillation columns, *Chem. Eng. Res. Des.* 99 (2015) 185–198.

[20] M.J. Lockett, Distillation Tray Fundamentals, first ed., Cambridge University Press, Cambridge, 2009.
[21] A.W. Dowling, L.T. Biegler, Rigorous optimization-based synthesis of distillation cascades without integer variables. Computer Aided Chemical Engineering, Elsevier, 2014.
[22] J.M. Douglas, Conceptual Design of Chemical Processes, 1st ed., McGraw-Hill Science/Engineering/Math, New York, 1988.
[23] Y.J. Ma, Y.Q. Luo, X. Ma, T. Yang, D.L. Chen, X.G. Yuan, Fast algorithms for equation-oriented flowsheet simulation and optimization using pseudo-transient models, *Ind. Eng. Chem. Res.* 57 (42) (2018) 14124–14142.
[24] A.R. Ciric, D.Y. Gu, Synthesis of nonequilibrium reactive distillation processes by MINLP optimization, *AIChE J.* 40 (9) (1994) 1479–1487.
[25] W. Song, G. Venimadhavan, J.M. Manning, M.F. Malone, M.F. Doherty, Measurement of residue curve maps and heterogeneous kinetics in methyl acetate synthesis, *Ind. Eng. Chem. Res.* 37 (5) (1998) 1917–1928.
[26] R. Taylor, R. Krishna, Modelling reactive distillation, *Chem. Eng. Sci.* 55 (22) (2000) 5183–5229.
[27] J.M. van Baten, J. Ellenberger, R. Krishna, Hydrodynamics of reactive distillation tray column with catalyst containing envelopes: experiments *vs.* CFD simulations, *Catal. Today* 66 (2–4) (2001) 233–240.
[28] L. Asselineau, P. Mikitenko, J.C. Viltard, M. Zuliani, Reactive distillation process and apparatus for carrying it out, US. Pat. 5368691A (1994).
[29] D. Sanfilippo, M. Lupieri, F. Ancillotti, Process for preparing tertiary alkyl ethers and apparatus for reactive distillation, US. Pat. 5493059A (1996).

Appendix

Appendix A. Detailed TAC calculation for EG RD column

The equations for the TAC calculation were from Ciric and Gu [25] in this case. The optimization function includes the annualized cost of the column (COL), exchanger cost (EXC), feedstock cost (FEE) and downstream separation cost (SEP).

$$\mathrm{TAC} = \mathrm{COL} + \mathrm{EXC} + \mathrm{FEE} + \mathrm{SEP} \tag{A1}$$

The annualized cost of the column (COL):

$$\mathrm{COL} = c_{\mathrm{T}} D^{1.55} H + c_{\mathrm{SH}} D (H_0 + H)^{0.802} \tag{A2}$$

$$H = \sum_{j=1}^{N_s} e^j (H_{\min} + h_{\mathrm{w}}) \tag{A3}$$

where C_{T} is the cost parameter of trays. C_{SH} is the cost parameter of column shell. H represents column height. H_0 is the height of the column base, set to 9.84 ft (1 ft=0.3048 m). $H_{\min}$ is the minimum distance between the plates, set to 2 ft.

The exchanger cost (EXC):

$$\mathrm{EXC} = c_0 + c_{\mathrm{R}} Q_{\mathrm{R}} + c_{\mathrm{C}} Q_{\mathrm{C}} \tag{A4}$$

where c_0 is the cost parameters, c_{R} is heating utility cost, c_{C} is cooling utility cost, refer to Table A1 for specific values. Q_{R} and Q_{C} are the duty of the reboiler and the condenser, respectively.

The feedstock cost (FEE):

$$\mathrm{FEE} = (c_{\mathrm{EO}} \times F_{\mathrm{EO}} + c_{\mathrm{W}} \times F_{\mathrm{w}}) \cdot h_{\mathrm{year}} \tag{A5}$$

where F_{EO} and F_{W} are the feed flow rate of ethylene oxide and water respectively. c_{EO} and c_{W} are feedstock cost of ethylene oxide and water respectively. h_{year} is the annual working hour, the value here is 8000.

The downstream separation cost (SEP):

$$\mathrm{SEP} = c_{\mathrm{s}} \times L_{\mathrm{reb}} \times Z_{\mathrm{H_2O}} \times h_{\mathrm{year}} \tag{A6}$$

where c_{S} is downstream separation cost (USD·kmol^{-1} water in effluent). L_{reb} is the product stream. $Z_{\mathrm{H_2O}}$ is the mole fraction of water in the product stream.

Table A1
Parameters for economic evaluation

Parameter	Value
c_{T}/USD·a^{-1}	15.7
c_{SH}/USD·a^{-1}	222
c_0/USD·a^{-1}	10,000
c_{R}/USD·kW^{-1}·a^{-1}	146.8
c_{C}/USD·kW^{-1}·a^{-1}	24.5
c_{EO}/USD·kmol^{-1}	43.70
c_{W}/USD·kmol^{-1}	21.90
c_{S}/USD·kmol^{-1}	0.15

Appendix B. Detailed TAC calculation of MeOAc RD column

The equations for the TAC are calculated by Eq. (49) in this case. The equipment repayment period is 3 years. Energy consumption cost C_{energy} considers the cost of condenser and reboiler cold and hot utility consumption.

Column equipment cost:

$$C_{\mathrm{col,cap}} = C_{\mathrm{column}} + C_{\mathrm{plate}} \tag{B1}$$

$$C_{\mathrm{column}} = \left(\frac{\mathrm{M\&S}}{280}\right) 101.9 D^{1.066} H^{0.802} (2.18 + F_{\mathrm{c}}) \tag{B2}$$

$$F_{\mathrm{c}} = F_{\mathrm{M}} \times F_{\mathrm{P}} \tag{B3}$$

$$C_{\mathrm{plate}} = \left(\frac{\mathrm{M\&S}}{280}\right) 4.7 D^{1.55} H F_{\mathrm{c}} \tag{B4}$$

$$F_{\mathrm{c}} = F_{\mathrm{s}} + F_{\mathrm{t}} + F_{\mathrm{m}} \tag{B5}$$

where C_{column} and C_{plate} are column shell equipment cost and tray cost, respectively. M&S is the equipment cost factor, set to 1468.6. F_{c} is the correction factor. F_{M} and F_{P} are the correction factor for the container material and pressure, respectively, both of which are 1. In Eq. (B.5), the tray spacing coefficient F_{s} is set to 1, the tray type coefficient F_{t} is set to 0 for the sieve tray, and the material coefficient F_{m} is set to 0 for carbon steel.

Heat exchanger equipment cost:

$$C_{\mathrm{hx,cap}} = \left(\frac{\mathrm{M\&S}}{280}\right) 101.3 A^{0.65} (2.29 + F_{\mathrm{c}}) \tag{B6}$$

$$A = \frac{Q}{U \times \Delta T_{\mathrm{mean}}} \tag{B7}$$

$$F_{\mathrm{c}} = (F_{\mathrm{d}} + F_{\mathrm{p}}) F_{\mathrm{m}} \tag{B8}$$

$$\Delta T_{\mathrm{mean}} = \left[\left(T_{\mathrm{hot}}^{\mathrm{in}} - T_{\mathrm{cold}}^{\mathrm{out}}\right) \left(T_{\mathrm{hot}}^{\mathrm{out}} - T_{\mathrm{cold}}^{\mathrm{in}}\right) \left(T_{\mathrm{hot}}^{\mathrm{in}} - T_{\mathrm{cold}}^{\mathrm{out}} + T_{\mathrm{hot}}^{\mathrm{out}} - T_{\mathrm{cold}}^{\mathrm{in}}\right) \Big/ 2 \right]^{1/3} \tag{B9}$$

where A is the heat transfer area, ft^2. U is the heat transfer coefficient, which is 0.852 kW·K^{-1}·m^{-2} and 0.568 kW·K^{-1}·m^{-2} in the condenser and reboiler, respectively. Q is the heat duty of the reboiler or condenser. The selection of the reboiler adopts a kettle-type heat exchanger, and its correction factor F_{d} is 1.35. The type of condenser adopts fixed tube heat exchanger and its correction factor F_{d} is 0.8. The value of the pressure coefficient F_{p} is 0 when it is less than 1013.25 kPa. $T_{\mathrm{hot}}^{\mathrm{in}}$ and $T_{\mathrm{cold}}^{\mathrm{in}}$ are the temperature of the heat stream and cold stream entering the heat exchanger, respectively. Similarly, $T_{\mathrm{hot}}^{\mathrm{out}}$ and $T_{\mathrm{cold}}^{\mathrm{out}}$ are the temperature of the heat stream and cold stream exiting the heat exchanger, respectively.

Energy cost:

$$C_{energy} = h_{year} C_{ep} Q \quad \text{(B10)}$$

where C_{ep} is utility price. The utility prices used in this example case are shown in Table B1.

Table B1
Utility type and cost date.

Item	Value/USD·GJ^{-1}
Low pressure steam (600 kPa, 160 °C)	7.78
High pressure steam (1100 kPa, 254 °C)	9.88
Water (25–35 °C)	0.354